

REVEALING THE OBSCURED SUPERNOVA REMNANT KES 32 WITH CHANDRA

JACCO VINK^{1,2}

Columbia Astrophysics Laboratory, Columbia University, MC 5247, 550 W 120th street, New York, NY 10027, USA
j.vink@sron.nl

Draft version November 1, 2018

ABSTRACT

I report here on the analysis and interpretation of a *Chandra* observation of the supernova remnant Kes 32. Kes 32 is rather weak in X-rays due to a large interstellar absorption, which is found to be $\sim 4 \times 10^{22} \text{ cm}^{-2}$, larger than previously reported. Spectral analysis indicates that the ionization age of this object is very young, with $n_e t \sim 4 \times 10^9 \text{ cm}^{-3} \text{ s}$, and a temperature of $kT_e \sim 1 \text{ keV}$. The X-ray emission peaks at a smaller radius than in the radio. The low ionization age suggests that Kes 32 is a young remnant. However, a young age is in contradiction with the relatively large apparent size, which indicates an age of several thousand years, instead of a few hundred years. This problem is discussed in connection with Kes 32's unknown distance and its possible association with the Norma galactic arm.

Subject headings: X-rays: observations individual (Kes 32) – supernova remnants

1. INTRODUCTION

Green's catalog of supernova remnants³ lists 231 galactic supernova remnants. Most of them have been discovered in the radio (e.g. Kesteven 1968; Whiteoak & Green 1996), and the X-ray properties of only a fraction of them are well known. The reason is that most remnants lie in the galactic plane, where the X-ray emission is often absorbed by intervening matter. This is unfortunate, as X-ray emission can be very revealing about the nature of a supernova remnant. For example, the absence or presence of X-ray line emission, will reveal whether a remnant is X-ray synchrotron dominated, or dominated by a thermal emission. If X-ray line emission is observed, one can better determine the remnants evolutionary stage than with radio observations.

The launches of *Chandra* and *XMM-Newton* have given us the opportunity to improve our knowledge of the X-ray properties of obscured remnants, as they, unlike e.g. *ROSAT*, also cover $\sim 2 - 8 \text{ keV}$ spectral band, where X-ray absorption is less of a problem. Moreover, especially *Chandra* has good spatial resolution. Although in some cases the statistics may be limited, a high spatial resolution helps to remove contamination by point sources, and observations of complex fields are less affected by stray light from bright sources outside the field of view. This was sometimes a problem with *ASCA*, which covered the same spectral range as *Chandra*.

Here I report on the *Chandra* observation of one of those X-ray obscured remnants, Kes 32 (G332.4+0.1, MSH 16-51). It was proposed for observation with *Chandra*, as radio maps (Roger et al. 1985; Whiteoak & Green 1996) show that it has an interesting shell-type morphology, with a "blow out" on the eastern side, reminiscent of Cas A. Moreover, its size of $16'$ makes it a good *Chandra* target, since it just fits into the $17'$ field of view of the ACIS-I CCD detector.

Kes 32 is situated in a complicated field of the sky. At its location our line of sight is tangential to the "Norma" spiral arm (Fig. 1). Southwest lies the remnant G332.0+0.2, and $30'$ southeast of Kes 32 is the well known supernova remnant RCW 103

(G332.4-0.4, Fig. 2). A radio map of Kes 32 and its surroundings shows what looks like a jet emanating from the "blow-out" and connecting to a plume of diffuse emission (Roger et al. 1985). Although, intriguing, the "jet" and diffuse emission have a flat radio spectrum, suggesting unrelated thermal emission. This interpretation is also supported by $60 \mu\text{m}$ IRAS images (Whiteoak & Green 1996).

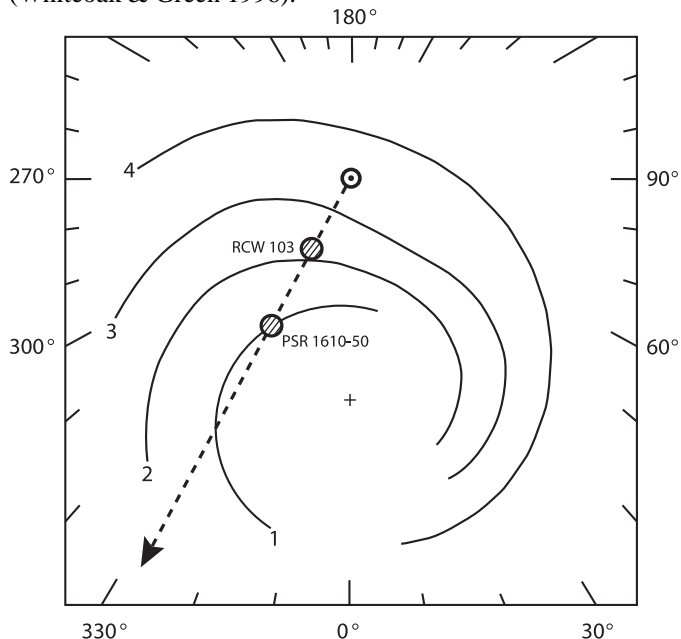


FIG. 1.— The direction of Kes 32 with respect to the spiral arms is indicated by the arrow. No. 1 is the "Norma" arm, no. 2 is the "Scutum-Crux" arm, and no. 3 the "Carina" arm. This figure is adapted from a figure in Taylor & Cordes (1993).

As it is interesting to place Kes 32 in the context of its surrounding, I show here the *ROSAT*-PSPC image of the remnants field twice (Fig. 2): one to indicate the positions of interesting

¹ Chandra fellow

² Present address: SRON National Institute for Space Research, Sorbonnelaan 2, 3584 CA Utrecht, The Netherlands

³ Online available at <http://www.mrao.cam.ac.uk/surveys/snrs/>. A printed summary can be found in Stephenson & Green (2002)

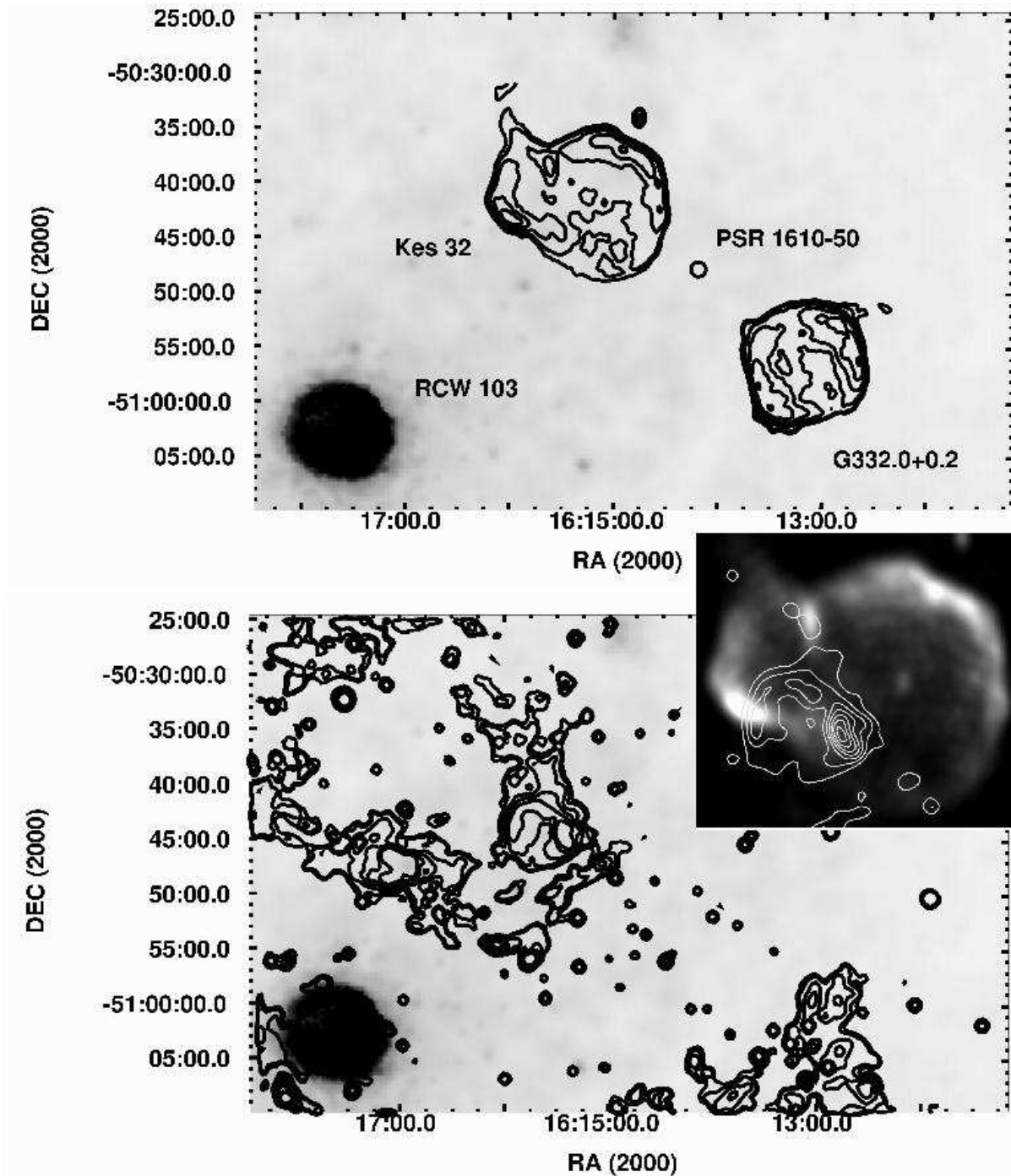


FIG. 2.— *ROSAT*-PSPC image of the field around Kes 32 (see Brinkmann et al. 1999). The X-ray image of RCW 103 is highly saturated in order to show the low level of X-ray background fluctuations. The first panel shows, with the help of radio contours how the remnants RCW 103 (saturated), Kes 32, and G332.0+02 are situated with respect to one another. The second panel displays infrared contours taken from a *MSX* A-band image ($8.3 \mu\text{m}$, contour levels 7, 7.5, 9, 11, and $15 \times 10^{-6} \text{ W m}^{-2} \text{sr}^{-1}$). The inset shows in more detail that the peak infrared emission coincides with the southeast of the remnant (here a radio map is shown), but is morphologically unrelated.

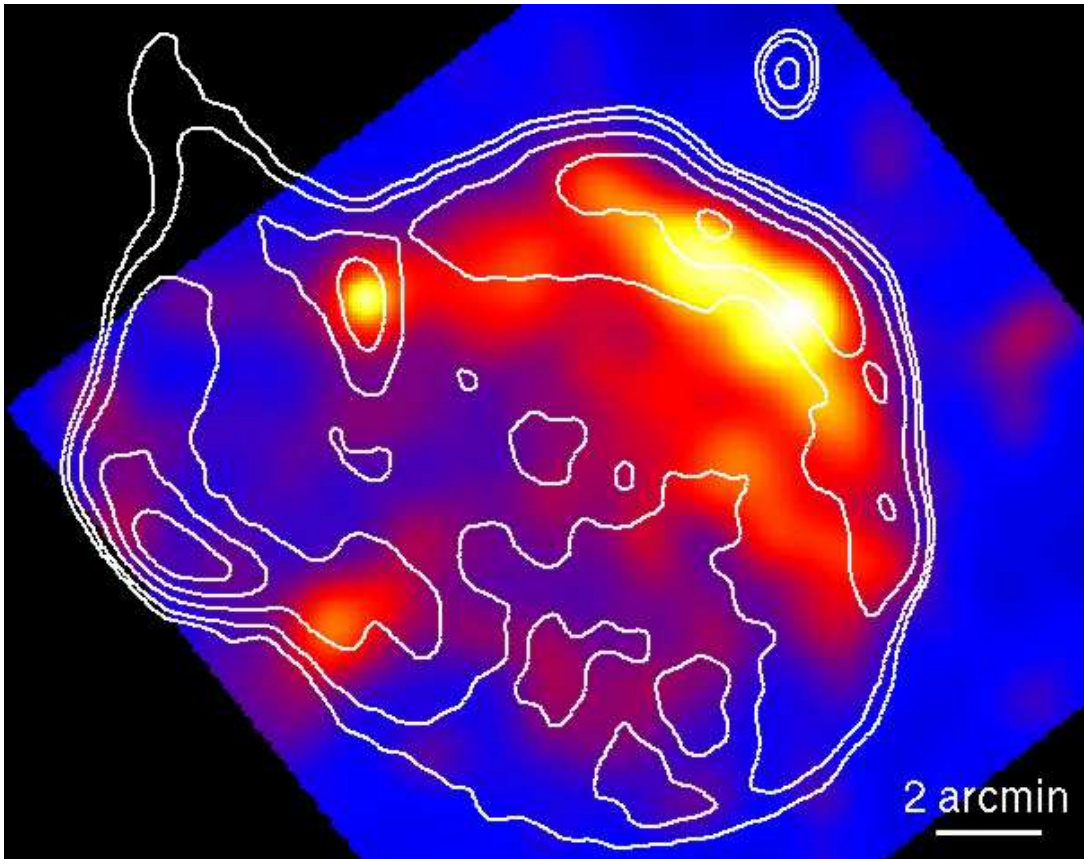


FIG. 3.— Adaptively smoothed Chandra ACIS-I image (1.6–3.5 keV) of Kes 32 with MOST 843 MHz radio contours overlaid (Whiteoak & Green 1996). The X-ray peak value is ~ 1 count per $5''$ pixel.

objects in the field, and one with the $8 \mu\text{m}$ *MSX* contours.⁴ The *ROSAT* image shows no obvious sign of Kes 32 or G332.0+0.2 (c.f. Brinkmann et al. 1999), but as is clear from the *MSX* contours, there is extended diffuse infrared emission over a large area. A shell-like structure with a radius of $\sim 3'$ coincides with Kes 32. However, the infrared shell is much smaller than Kes 32 and has a different morphology, which makes it unlikely that the infrared source is physically connected to the remnant.

Given Kes 32’s location, chance alignments with other interesting sources are to be expected. The proximity of the young radio pulsar PSR 1610-50 is probably coincidental, although it was proposed by Caraveo (1993) to be physically associated with Kes 32. There is no morphological connection between Kes 32 and PSR 1610-50, and there are no indications for the presence of a bow-shock, which one might expect for a high velocity pulsar that has escaped the associated supernova remnant (Pivovarov et al. 2000; Stappers et al. 1999).

In this article I concentrate on the X-ray properties of Kes 32, and as I will show, its X-ray spectral and morphological properties suggest Kes 32 to be a young remnant, but this is somewhat in conflict with its size, especially if Kes 32 is situated in the “Norma” arm.

2. OBSERVATION AND DATA REDUCTION

Kes 32 was observed by the *Chandra* observatory as part of

its guest observer program on October 20, 2001. The prime instrument was ACIS-I, which was operated in “faint” mode. The data were reduced with the standard *Chandra* software CIAO v. 2.3. In order to keep up with the improved instrumental calibration, a new CTI corrected photon event list was created from the raw event list. In addition, time intervals with increased background levels were excluded, resulting in an effective exposure time of 29 ks.

Kes 32 is a rather X-ray faint supernova remnant, and only after smoothing or rebinning of the raw image can one obtain an appealing X-ray map. As will be explained below, Kes 32 is also heavily absorbed and only above ~ 1.5 keV is it detectable in X-rays. Fig. 3 therefore shows an adaptively smoothed *Chandra* image for the approximate energy range 1.6–3.5 keV. The smoothing was done on the count image after the removal of point sources. The effective resolution of the resulting image is roughly $15''$. The overlaying contours show the radio emission obtained from the MOST map.⁵

Kes 32 was first detected in X-rays by *ASCA* (Kawai et al. 1998), but the *Chandra* image in Fig. 3 is a clear improvement over the *ASCA* X-ray map (Kawai et al. 1998; Pivovarov et al. 2000). It shows that the X-ray morphology is not unlike the radio morphology, with a broken shell that is brighter in the northwest. The relatively bright southeastern part of the radio shell is absent in the X-ray image. One should, however,

⁴ Infrared maps obtained by the US Air Force Midcourse Space Experiment (*MSX*) can be downloaded from <http://www.ipac.caltech.edu/ipac/msx/msx.html>.

⁵ Radio images of supernova remnants from the Whiteoak & Green (1996) MOST catalog can be downloaded from “NCSA Astronomy Digital Image Library (ADIL)”, <http://adil.ncsa.uiuc.edu/>

be aware that, as Kes 32 lies very close to the galactic plane, spatial variations in the absorption may influence the observed X-ray morphology.

A more remarkable difference between the radio and X-ray maps is that the northern part of the shell seems to have a smaller radius in X-rays than in the radio. This is more clearly illustrated in Fig. 4, which shows that the peak of the X-ray emission is shifted by $\sim 1'$ with respect to the radio emission. An explanation may be that the X-ray emission, which is dominated by line emission, is mainly coming from metal rich ejecta, whereas the radio emission is coming from shocked swept up matter. This would imply that Kes 32 is an ejecta rich, and therefore young, supernova remnant.

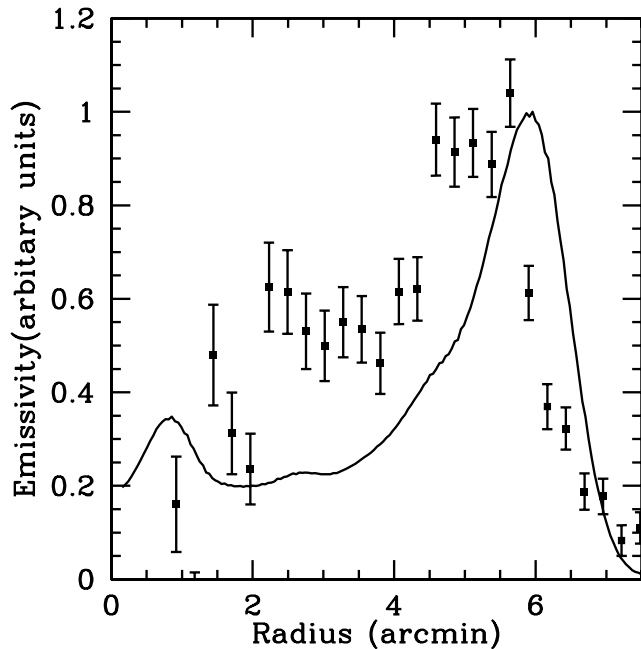


FIG. 4.— Radial X-ray (data points) and radio emissivity (line) profiles, azimuthally integrated from west to north centered on $\alpha_{J2000} = 16\text{h}15\text{m}10.4\text{s}$, $\delta_{J2000} = -50^{\circ}42'21.4''$. The X-ray profile is based on the unsmoothed *Chandra* image.

However, an alternative explanation is that the electron temperature is cooler near the edge of the remnant. As the emission from cool plasma is more absorbed, it will not show up in the X-ray image. From a theoretical point of view it is hard to predict whether to expect such a temperature gradient. The self-similar hydrodynamical models by Chevalier (1982), which are applicable to young remnants, actually predict a cool inner shell and a hot outer shell. The well known Sedov model on the other hand predicts a shell around an hot interior, but the interior is so tenuous that almost all X-ray emission comes from the shell. To complicate things, it is becoming increasingly clear that the electron temperature, which determines the X-ray emission properties, is often cooler than the dynamically more important proton temperature (e.g. Vink et al. 2003). Also observationally there is no unambiguous evidence for radial temperature gradients in supernova remnants. In Cas A there is evidence that the temperature near the shock front is higher than in the bright inner shell (e.g. Fabian et al. 1980; Vink & Laming 2003), whereas the presence of Fe K emission from the interior of Tycho indicates an hot interior (Hwang & Gotthelf 1997; Decourchelle et al. 2001).

3. SPECTROSCOPY

The *ASCA* CCD spectrum of Kes 32 revealed for the first time X-ray emission lines of silicon, sulfur and argon. Kawai et al. (1998) reported that the fitted temperature was higher than 4 keV and a low ionization parameter ($n_e t$), which they did not further quantify. For the same data Brinkmann et al. (1999) reported an absorbing column of $N_{\text{H}} = 5 \times 10^{21} \text{ cm}^{-2}$. The *Chandra* spectrum of Kes 32 also shows prominent Si and S lines, and the spectrum is best fitted with an underionized plasma (Fig. 5, Table 1), but the absorbing column is probably much higher, and the temperature lower, than reported by Brinkmann et al. (1999) and Kawai et al. (1998). However, this conclusion depends on the method of background subtraction.

I only fully analyzed the *Chandra* spectrum extracted from the Northwestern part of the shell (Fig. 6), which has the highest signal to noise ratio. For the background correction two methods were compared: extracting a background spectrum from the observation itself, using the border of the field of view (see Fig. 6), or by extracting a spectrum from the standard *Chandra* blank sky data. As both Fig. 5 and Fig. 7 indicate, the local background spectrum is very different from the standard background spectrum, especially below 2 keV. Some disadvantages of using the local background, namely the dependence on detector region due to vignetting effects, and different ratios between particle and photon background, can be overcome by using a scheme explained by Arnaud et al. (2002). In this method both the source and the local background spectrum are corrected with blank field data from the appropriate detector regions. This results in a source spectrum that is only contaminated by local background, and a local background spectrum specific for Kes 32 that has been corrected for contamination by global effects like particle background. In order to correct the background spectrum for the effects of vignetting, an energy dependent correction factor was applied, based on the ratio of effective area for the source position versus the background extraction region. The correction factors were calculated from the weighted auxiliary response files (ARFs) for the background and source regions, obtained with the CIAO tool *acispec*. Another correction factor corrects for the different sizes of the extraction regions.

Using this corrected local background spectrum gives a goodness of fit of $\chi/\nu = 107.1/64$ (Table 1). Including an additional hot component, fixed at $kT_e = 3.5$ keV, does not substantially improve the fit ($\Delta\chi^2 = 7$ for 2 additional degrees of freedom), nor does it significantly change the parameters of the dominant soft component. The 1.5-5 keV luminosity of such a hot component is more than a factor ten below that of the cooler component.

Inspecting the local background spectrum reveals a dominant excess emission above the blank sky background between 0.7 and 1.4 keV, which is neither visible in the blank sky background, nor in the background corrected spectrum of Kes 32. As the background spectrum was extracted after the removal of point sources (there were only a few bright point sources), the excess soft emission is probably diffuse.

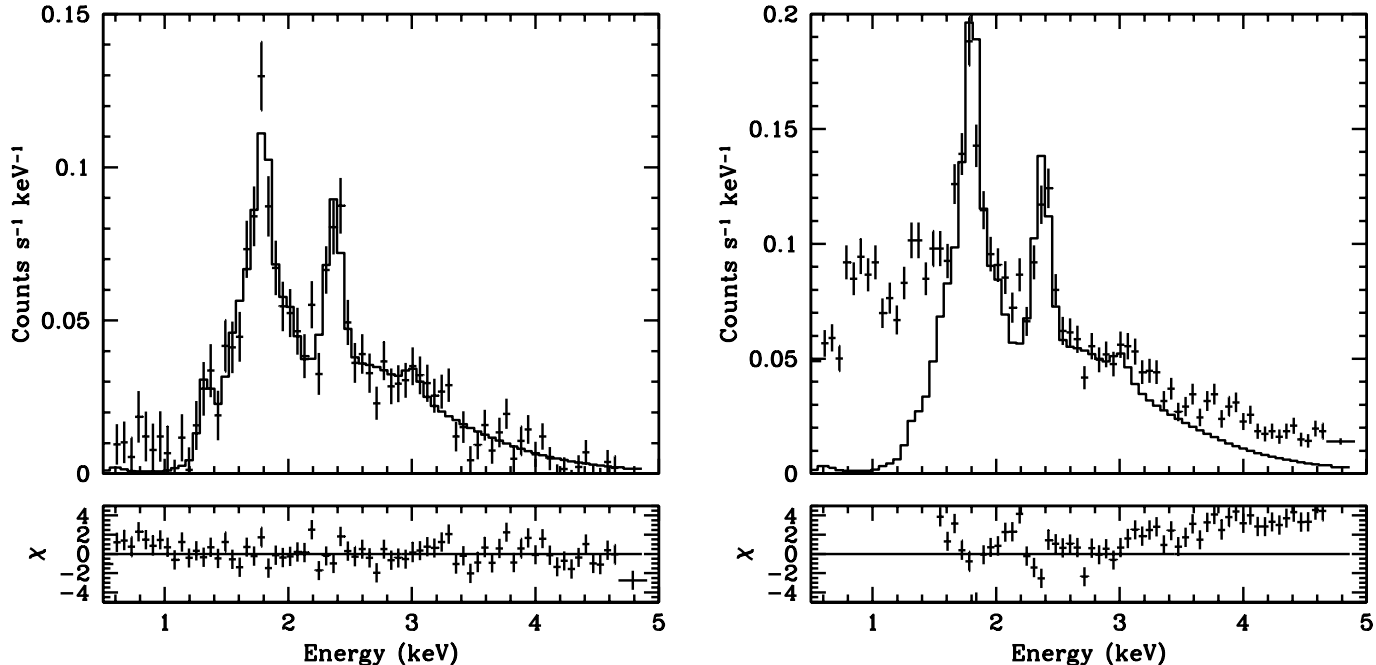


FIG. 5.— The *Chandra* ACIS-I spectrum of the bright northwestern shell of Kes 32. The spectrum on the left is background corrected with the locally extracted background, on the right with the standard blank sky background. The solid lines indicate the best fit model corresponding to “method 1” in Table 1, but has been scaled to fit the hard X-ray spectrum in the spectrum on the right, in order to reveal the soft X-ray excess, which is probably due to foreground emission.

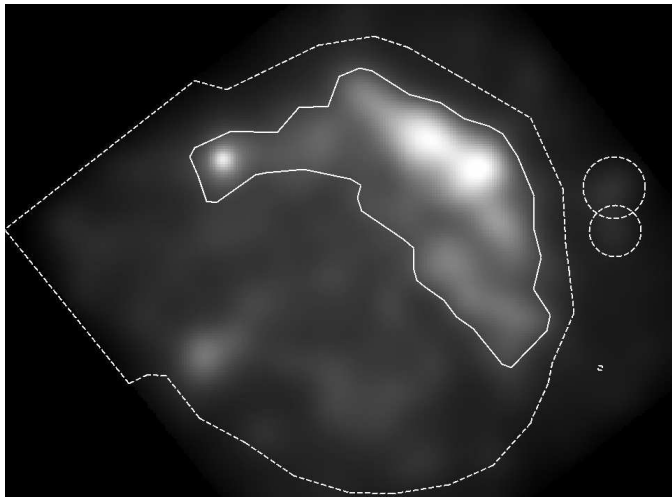


FIG. 6.— Gray scale version of Fig. 3 with the spectral extraction regions overlaid. The solid line indicates the source extraction region. For the extraction of the background spectrum the complete field of view of the ACIS-I detector was used, excluding the regions indicated by the dotted lines. (the dotted polygon follows the outer contour of the radio map, for as far as it lies within the ACIS-I detector).

The presence of excess soft emission is not surprising, given Kes 32’s position in a crowded region in the galaxy. The fact that the remnant is heavily absorbed, indicates that the soft X-ray excess is due to foreground emission. Local foreground emission in that direction also helps explain why Kawai et al. (1998) measured a relatively low absorption, whereas on the other hand the soft X-ray morphology observed by *ROSAT* (Brinkmann et al. 1999) is uncorrelated with the *ASCA* morphology.

Although correcting the spectrum with a locally extracted background spectrum has the disadvantage that it comes from

a different detector region, it gives a better assessment of the Kes 32’s X-ray spectrum. However, above 1.5 keV the local foreground emission is less important. I therefore include in Table 1 a column with the results for the spectrum corrected with the standard blank sky background, but excluding data below 1.5 keV. Both spectra are modeled with single temperature non-equilibrium ionization (NEI) models. As the spectral range and the statistical quality of the data is rather limited, a single temperature model is sufficient for the analysis of the spectra, but in reality temperature gradients are likely to be present.

Although there are obvious differences in fit parameters for using the two different background subtraction methods, which serves to emphasize the systematic uncertainties involved in a study like this, qualitatively the results are similar. Both fits indicate a lower temperature, ~ 1 keV, and a much higher absorption column of $N_{\text{H}} \sim 4 \times 10^{22} \text{ cm}^{-2}$ than previously reported. Remarkable is also the factor 8 difference in the Si and S abundance. It is hard to believe that this reflects the true, overall, difference in Si and S abundances, as both elements are oxygen burning products. More plausible is that most of the Si is contained in dust. Another explanation may be that the absorption model (Morrison & McCammon 1983) is not adequate for Kes 32. For the absorption values reported here, the absorption by intervening Si is important and uncertainties in the atomic data or the state of the absorbing material may have affected the measured Si abundance.

It is not clear to me why the *ASCA* observation indicate a much higher temperature. It may be related to the differences in background subtractions. Moreover, Kes 32 is in a crowded field and it is possible that stray light from bright objects outside the field of view have contaminated the *ASCA* source spectrum, as the *ASCA* mirrors cause more stray light problems. The remarkably low ionization parameters is, however, also found with *ASCA* (Tamura private communication). From a statisti-

cal point of view the low ionization parameter is significant; even a 4σ parameter range indicates that $n_e t < 2 \times 10^9 \text{ cm}^{-3}\text{s}$. The fact that also *ASCA* observation supports a low ionization parameter makes it unlikely that it is caused by calibration errors. However, I cannot totally exclude it, as gain errors may result in small energy shifts. The low ionization parameter is determined from the absence of hydrogen-like Si and S emission, and from the energy centroid of the Si and S emission. In particular the centroid energies are sensitive to calibration problems. Although the spectral resolution of the ACIS-I instrument has deteriorated with time, the instrument is regularly calibrated, and according to information on the *Chandra* website the gain is accurate to about 0.3%, with most uncertainties at energies below 1.2 keV, which are not relevant for the highly absorbed spectrum of Kes 32.

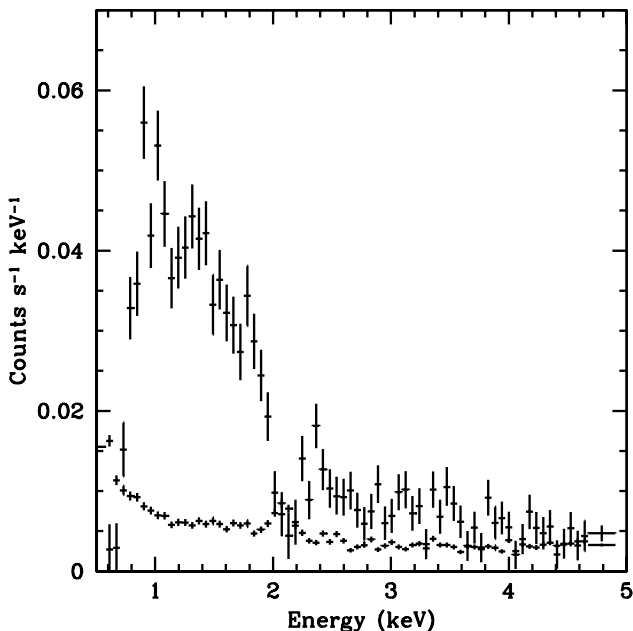


FIG. 7.— A comparison of the locally extracted background spectrum from the ACIS-I instrument and the background extracted from the standard *Chandra* blank sky fields.

Finally, I extracted a spectrum from the bright spot to the north of the opening in the shell, which is the location from which a jet-like feature seems to emanate in the radio map of Roger et al. (1985). The idea was to find evidence for spectral differences between this spot and the rest of the shell, that might support the presence of a “jet”. However, the statistics of the extracted spectrum was too poor, and both a power law model, or the best fit NEI model for the rest of the shell fit the spectrum.

4. DISCUSSION

I have presented the results of a *Chandra* observation of Kes 32. Although the statistical quality is limited, the resulting X-ray image is a clear improvement over the existing *ASCA* map. The spectral analysis of the data indicates that some of the X-ray emission below 1.5 keV should be attributed to diffuse foreground emission. The low ionization parameter suggests that Kes 32 is young, or is evolving in a low density region. The average density of the remnant can be expressed as $n_H = 1.5 \times 10^{-7} \sqrt{\varepsilon/f d_5} \text{ cm}^{-3}$, with ε the emission measure

as defined in Table 1, f the volume fraction, and d_5 the distance in units of 5 kpc. Note that n_H does not depend strongly on the adopted distance or volume fraction. As the emission measures only apply to about half of the remnant, I use $f = 0.15$, which gives a density of roughly $0.6 - 1.3 \sqrt{1/d_5} \text{ cm}^{-3}$. This is surprisingly high given the low ionization parameter, and implies an age of ~ 300 yr. Such a young age is not unreasonable given the measured S overabundance, and the X-ray radius being smaller than the radio radius, which possibly indicates the presence of an X-ray emitting ejecta shell.

However, Kes 32 has a radius of $\sim 8'$ which is difficult to reconcile with a young age, certainly if the distance is as large as 8 kpc. Such a large distance to Kes 32 should be considered, given the large column density. A lower limit to the distance is provided by the nearby source RCW 103, which has smaller absorption column of $N_H \sim 7 \times 10^{21} \text{ cm}^{-2}$ (Gotthelf et al. 1999), and is at a distance of 3.3 kpc (Caswell et al. 1975). As is illustrated in Fig. 1, RCW 103 is likely located in or near the “Crux” spiral arm. It is possible that Kes 32 is at the far side of the “Crux” arm, at roughly 3.5 kpc, and RCW 103 on the near side, but given the high column density and the fact that the supernova remnant density is expected to be high where the line of sight is tangential to a spiral arm, an association of Kes 32 with the “Norma” arm seems very reasonable. In that case the distance range is 7.5–11 kpc, in agreement with OH absorption measurements indicating a distance > 6.6 kpc (Caswell & Haynes 1975). For this distance range, the angular radius of $\sim 8'$ corresponds to 17 pc to 25 pc. This is very large for a 300 yr old remnant; it requires an average shock velocity of $40,000 \text{ km s}^{-1}$, too fast for a typical young remnant, unless it is the result of an hypernova explosion. Even for a distance of 3.3 kpc the average velocity still measures $24,000 \text{ km s}^{-1}$. It is therefore more plausible that the ionization age does not reflect the actual age very well. This could, for example, be the result of a supernova explosion in a low density, wind blown, cavity. This produces a faint supernova remnant until the blast wave hits the denser material swept up by the wind. It then brightens and evolves rapidly (Tenorio-Tagle et al. 1991). This means that, although the remnant may be older, most of the plasma has been shocked relatively recently, resulting in a low ionization age. Such a scenario has been proposed for the supernova remnant RCW 86, in order to explain the low ionization age of parts of that remnant (Vink et al. 1997). A more reasonable average shock velocity of 5000 km s^{-1} , gives an age of ~ 3000 yr for a distance of 7.5 kpc.

The distance to Kes 32 is of some interest as a distance of 7.5 kpc would bring it close to pulsar PSR 1610-50. Pivovarov et al. (2000) disputed a physical association between the pulsar and Kes 32 on the grounds of absence of X-ray emission from a bow shock, which implies an upper limit to the velocity of 170 km s^{-1} . To that argument may be added that the young age of Kes 32, or its rapid evolution inside a cavity in the interstellar medium, imply a high average shock velocity. However, given the large X-ray absorption to Kes 32 the absence of an X-ray bow shock around PSR 1610-50 may not be a conclusive argument for not associating Kes 32 with the pulsar.

In conclusion: *Chandra*’s observation of Kes 32 confirms its young spectral age and reveals it to be more obscured than previously thought. The absorbing column of $\sim 4 \times 10^{22} \text{ cm}^{-2}$ indicates a large distance, but as this also means a large shock radius, this is hard to reconcile with the idea that Kes 32 is a young remnant. New X-ray observations may be able to un-

cover more of Kes 32 from under its shroud of absorption and solve the age/size paradox. A higher throughput and, especially, a higher spectral resolution, will result in a more accurate estimate of the ionization age and abundance of the remnant. However, this requires a much deeper X-ray observation, for instance with *XMM-Newton*, or it has to wait for the next generation of high throughput X-ray observatories, such as Constellation-X, which will also contain high resolution spectrometers.

I thank the anonymous referee, whose suggestions helped improved this article. This work is supported by the NASA through Chandra Postdoctoral Fellowship Award Number PF0-10011 and by Chandra Award GO1-2059X issued by the Chandra X-ray Observatory Center, which is operated by the Smithsonian Astrophysical Observatory for NASA under contract NAS8-39073. This study has profited from data obtained from the ROSAT Data Archive at MPE, the NASA/IPAC Infrared Science Archive, and NCSA Astronomy Digital Image Library archival facilities.

REFERENCES

- Anders, E. & Grevesse, N. 1989, *Geochim. Cosmochim. Acta*, 53, 197
 Arnaud, M. et al. 2002, *A&A*, 390, 27
 Brinkmann, W., Kawai, N., Scheingraber, H., Tamura, K., & Becker, W. 1999, *A&A*, 346, 599
 Caraveo, P. A. 1993, *ApJ*, 415, L111+
 Caswell, J. L. & Haynes, R. F. 1975, *MNRAS*, 173, 649
 Caswell, J. L., Murray, J. D., Roger, R. S., Cole, D. J., & Cooke, D. J. 1975, *A&A*, 45, 239
 Chevalier, R. A. 1982, *ApJ*, 258, 790
 Decourchelle, A. et al. 2001, *A&A*, 365, L218
 Fabian, A. C., Willingale, R., Pye, J. P., Murray, S. S., & Fabbiano, G. 1980, *MNRAS*, 193, 175
 Gotthelf, E. V., Petre, R., & Vasisht, G. 1999, *ApJ*, 514, L107
 Hwang, U. & Gotthelf, E. V. 1997, *ApJ*, 475, 665
 Kaastra, J. S., Mewe, R., & Nieuwenhuijzen, H. 1996, in *Proc. of the 11th Coll. on UV and X-ray, UV and X-ray Spectroscopy of Astrophysical and Laboratory Plasmas*, ed. K. Yamashita & T. Watanabe (Tokyo:Universal Academy Press), 411
 Kawai, N., Tamura, K., & Saito, Y. 1998, *Advances in Space Research*, 21, 213
 Kesteven, M. J. L. 1968, *Australian Journal of Physics*, 21, 369
 Morrison, R. & McCammon, D. 1983, *ApJ*, 270, 119
 Pivovarov, M. J., Kaspi, V. M., & Gotthelf, E. V. 2000, *ApJ*, 528, 436
 Roger, R. S., Milne, D. K., Kesteven, M. J., Haynes, R. F., & Wellington, K. J. 1985, *Nature*, 316, 44
 Stappers, B. W., Gaensler, B. M., & Johnston, S. 1999, *MNRAS*, 308, 609
 Stephenson, F. R. & Green, D. A. 2002, *Historical supernovae and their remnants* (Oxford: Clarendon Press)
 Taylor, J. H. & Cordes, J. M. 1993, *ApJ*, 411, 674
 Tenorio-Tagle, G., Rozyczka, M., Franco, J., & Bodenheimer, P. 1991, *MNRAS*, 251, 318
 Vink, J., Kaastra, J. S., & Bleeker, J. A. M. 1997, *A&A*, 328, 628
 Vink, J. & Laming, J. M. 2003, *ApJ*, 584, 758
 Vink, J., Laming, J. M., Gu, M. F., Rasmussen, A., & Kaastra, J. 2003, *ApJ*, 587, 31
 Whiteoak, J. B. Z. & Green, A. J. 1996, *A&AS*, 118, 329

TABLE 1
BEST FIT NEI MODELS.

Parameter	method 1	method 2
$n_{\text{H}} n_e V / 4\pi d^2 (10^{12} \text{ cm}^{-5})$	$17 + 20 / - 9$	2.4 ± 0.7
kT_e (keV)	0.61 ± 0.09	1.34 ± 0.14
$n_e t (10^9 \text{ cm}^{-3} \text{ s}^{-1})$	$5.3 + 3.2 / - 1.9$	3.2 ± 0.9
Mg	$1.4 + 2.4 / - 0.9$	-
Si	0.7 ± 0.4	0.42 ± 0.17
S	4.6 ± 2.5	3.8 ± 1.0
Ar	$10 + 14 / - 10$	$0.4 + 3.8 / - 0.4$
$N_{\text{H}} (10^{22} \text{ cm}^{-2})$	5.6 ± 0.8	3.1 ± 0.4
χ^2 / ν	107.1/64	116/48
$L_X^a (10^{34} \text{ erg s}^{-1})$	2.9	1.8
$F_X^a (10^{-12} \text{ erg s}^{-1} \text{ cm}^{-2})$	1.2	2.4

Note. — Model fits were made with the *SPEX* 1.10 X-ray spectral code (Kaastra et al. 1996). The method 1 and 2 columns give parameters for the same source spectrum, but with different background subtraction methods, as explained in the text; background 1 is extracted from the same observation, 2 is extracted from the standard *Chandra* background fields, but the spectrum was only fitted for energies > 1.5 keV. Abundances are given with respect to the cosmic abundances of Anders & Grevesse (1989); errors were calculated using $\Delta\chi^2 = 2.7$ (90% confidence).

^aThe unabsorbed flux, F_X , and luminosity at a distance of 5 kpc, L_X , are given for the spectral range 1.5-5 keV.